AGU PUBLICATIONS

Global Biogeochemical Cycles

RESEARCH ARTICLE
10.1002/2013GB004595

Key Points:
- We modeled soil C and N flux with various microbial parameters and structures
- Mineralization rates were validated with lab incubation data from diverse soils
- Inclusion of microbial biomass and C:N stoichiometry improves global models

Supporting Information:
- Readme
- AppendixA_fs01fs02.docx
- AppendixB_fs03.docx
- AppendixC_fs04.docx
- AppendixD_fs05.docx
- AppendixE_fs06.docx
- AppendixF_fs07.docx
- AppendixG_fs08.docx
- ts01.xlsx

Correspondence to:
Y. Fujita,
Yuki.Fujita@kwrwater.nl

Citation:
Fujita, Y., J.-P. M. Witte, and P. M. van Bodegom (2014), Incorporating microbial ecology concepts into global soil mineralization models to improve predictions of carbon and nitrogen fluxes, *Global Biogeochem. Cycles*, *28*, doi:10.1002/2013GB004595.

Received 26 FEB 2013
Accepted 15 FEB 2014
Accepted article online 17 FEB 2014

Incorporating microbial ecology concepts into global soil mineralization models to improve predictions of carbon and nitrogen fluxes

Yuki Fujita[1], Jan-Philip M. Witte[1,2], and Peter M. van Bodegom[2]

[1]Team Ecohydrology, KWR Watercycle Research Institute, Nieuwegein, Netherlands, [2]Department of Ecological Science, subdepartment of Systems Ecology, Vrije Universiteit, Amsterdam, Netherlands

Abstract Global models of soil carbon (C) and nitrogen (N) fluxes become increasingly needed to describe climate change impacts, yet they typically have limited ability to reflect microbial activities that may affect global-scale soil dynamics. Benefiting from recent advances in microbial knowledge, we evaluated critical assumptions on microbial processes to be applied in global models. We conducted a sensitivity analysis of soil respiration rates (*Cmin*) and N mineralization rates (*Nmin*) for different model structures and parameters regarding microbial processes and validated them with laboratory incubation data of diverse soils. Predicted *Cmin* was sensitive to microbial biomass, and the model fit to observed *Cmin* improved when using site-specific microbial biomass. *Cmin* was less affected by the approach of microbial substrate consumption (i.e., linear, multiplicative, or Michaelis-Menten kinetics). The sensitivity of *Cmin* to increasing soil N fertility was idiosyncratic and depended on the assumed mechanism of microbial C:N stoichiometry effects: a C overflow mechanism upon N limitation (with decreased microbial growth efficiency) led to the best model fit. Altogether, inclusion of microbial processes reduced prediction errors by 26% (for *Cmin*) and 7% (for *Nmin*) in our validation data set. Our study identified two important aspects to incorporate into global models: site-specific microbial biomass and microbial C:N stoichiometry effects. The former requires better understandings of spatial patterns of microbial biomass and its drivers, while the latter urges for further conceptual progress on C-N interactions. With such advancements, we envision improved predictions of global C and N fluxes for a current and projected climate.

1. Introduction

Current concerns about climate change urge for robust estimates of greenhouse gas emissions on national to global scales [*IPCC*, 2007]. At the same time, regional and national policymakers keep seeking for better tools to assess N loading to ecosystems. The increasing number of global soil organic matter (SOM) models (i.e., models developed for global-scale application [in the sense of *Manzoni and Porporato*, 2009]) in the last decades mirrors this general interest for predictions of soil carbon (C) and nitrogen (N) fluxes on large spatial scales. These SOM models typically have simple mathematical formulations [*Manzoni and Porporato*, 2009], whereas validation of such models is generally limited due to the inherent difficulty of collecting data on a large spatial scale.

In parallel, recent advances in knowledge about soil microbial processes have led to major improvements in small-scale SOM models (i.e., models describing small-scale processes, e.g., microbiology, rhizosphere, and aggregate models [in the sense of *Manzoni and Porporato*, 2009]). From a mechanistic point of view, SOM decomposition is increasingly seen as an enzyme-catalyzed process by microbes rather than an entirely substrate-controlled process [*Fang et al.*, 2005; *Schimel and Weintraub*, 2003; *Sinsabaugh et al.*, 2008]. Accordingly, an increasing number of small-scale SOM models include microbes as a state variable, through which physiological characteristics of microbes can be readily incorporated. The explicit treatment of microbial biomass not only improved the ability of models to capture C dynamics in fluctuating environments (e.g., through varying soil moisture [*Lawrence et al.*, 2009] and upon varying substrate supply [*Blagodatsky and Richter*, 1998]) but also provided a tool to theoretically investigate how functionally different microbes affect decomposition of C [*Allison et al.*, 2010; *Allison*, 2012].

Including microbe-mediated processes also facilitates a better understanding of the link between C and N flows. The traditional way of seeing decomposition as a completely C-limited process evolves toward an

integrated treatment of C-N interactions via microbial stoichiometry [*Schimel and Weintraub*, 2003]. An increasing, but still limited, number of small-scale SOM models adopt mechanisms of soil N controlling C flows [*Manzoni and Porporato*, 2009], and a series of analytical studies revealed that C-N interactions strongly determine the dynamics in soil C [*Manzoni and Porporato*, 2007; *Porporato et al*., 2003]. Empirical studies also support the importance of C-N interactions for predicting litter decomposition rates [*Manzoni et al*., 2008; *Parton et al*., 2007]. A possible mechanism responsible for the microbe-mediated effect of N on C is altered microbial growth efficiency (MGE) (i.e., the fraction of microbial C uptake that is incorporated into new microbial biomass). For example, MGE tends to decrease with decreasing availability of litter substrate N [*Manzoni et al*., 2008]. In addition, a theoretical analysis showed that MGE predominantly determines the threshold of the substrate C:N ratio where soil switches from an N sink to an N source [*Manzoni et al*., 2010]. High sensitivity of MGE to other environmental factors such as temperature and moisture [*Frey et al*., 2013; *Manzoni et al*., 2012] further indicates that microbial control on C-N interactions could be dynamic and complex.

This knowledge on microbe-mediated processes is, however, seldom incorporated into SOM models applied to large spatial scales [*Ostle et al*., 2009; *Wieder et al*., 2013]. Simple, substrate-controlled linear functions are typically used in global SOM models [e.g., *Todd-Brown et al*., 2013]. Such functions are argued to be sufficient to describe decomposition processes in long-term SOM models [*Manzoni and Porporato*, 2007], since fluctuations of microbial biomass, which can be captured only when microbe-substrate relations are explicitly included, will be masked by other predominating variability (e.g., climate) in the long term. Because spatial and temporal scales of most SOM models are correlated, global models are usually built for long-term simulations and therefore employ linear decomposition functions. We may question, however, if the omission of microbial properties in global models is truly justified. On the one hand, one may argue that among-site variations in biotic and abiotic factors are so large that differences in microbial properties may be ignored. On the other hand, there is enough evidence that predominantly biomass and physiological characteristics of microbes drive the biogeochemical cycles of C and N [*Falkowski et al*., 2008]. The fact that, for instance, microbial biomass differs by almost an order of magnitude among biomes [*Fierer et al*., 2009] may thus have important implications for global C and N fluxes. Moreover, even slightly different assumptions on C:N stoichiometry effects result in contrasting predictions of soil C efflux [*Manzoni and Porporato*, 2009], implying that analytical and empirical investigation of the C-N coupling in global SOM models merits serious consideration. This underlies the increasing number of calls for integrating microbial activity into SOM models to predict responses to global change [e.g., *Bardgett et al*., 2008; *McGuire and Treseder*, 2010; *Todd-Brown et al*., 2011; *Wieder et al*., 2013]. However, empirical data on a broad range of conditions to parameterize and validate such models are critically lacking [*Treseder et al*., 2012], which hampers a judgment of how much and where current models need to be improved [*Todd-Brown et al*., 2011].

Therefore, this study aims at evaluating the need to incorporate knowledge from microbial ecology into SOM models for predicting soil C and N fluxes across different soil conditions. For simplification, throughout this paper, we consider short-term fluxes from soils at steady-state conditions, without their long-term dynamical changes. To meet our research aim, we examined (using a simple process-based SOM model modified from CENTURY) whether incorporating small-scale microbial processes and microbial parameters improves across-site predictions of soil respiration and N mineralization rates. First, we tested the sensitivity of soil respiration and N mineralization rates to model parameter values of microbes (microbial biomass, microbial growth efficiency, microbial C:N ratio) under different model structures (i.e., three approaches of microbial substrate consumption kinetics and four presumed mechanisms of microbial C:N stoichiometry effects on C fluxes). Second, we validated the model outputs with empirical data obtained from laboratory incubation experiments of various soils. This allowed us to investigate whether inclusion of site-specific microbial data improves the model prediction across sites and which model structures seem generally most appropriate. Finally, we infer from our findings how global models can be improved by incorporating knowledge of microbial ecology, in terms of its variation in parameters and of its approaches, to allow more robust predictions of soil effluxes upon global change.

2. Methods

2.1. Model Approaches

We base our modeling framework on CENTURY [*Parton et al*., 1987], a commonly applied SOM decomposition model on large spatial (i.e., across-ecosystems) scale. Predicted carbon pools and fluxes of CENTURY have

been well validated with empirical data sets across ecosystems [e.g., *Kelly et al*., 2000; *Schimel*, 1994]. Moreover, CENTURY is simple enough to evaluate the components that we were interested in, while concepts similar to those in CENTURY are applied in most if not all global models.

CENTURY consists of three carbon pools with contrasting decomposition rates (i.e., active, slow, and passive pools). The active pool implicitly represents living microbes and microbial products, with microbes accounting for approximately one half to one third of carbon mass in the active pool [*Parton et al*., 1993]. Here we modified CENTURY to explicitly represent microbes, by splitting the active pool into a microbial pool and an easily decomposable substrate pool. For simplicity, we merged the slow and passive pools of CENTURY into one recalcitrant substrate pool. Parameter values were adjusted so that C flows remained realistic and equal to those in default CENTURY settings (see Appendix A for a full description about the model modifications). Table 1 summarizes all abbreviations of variables and parameters used in our model.

In most SOM models, the decomposition rate of the substrate is described in relation to microbes and substrate, as it is a process of microbes consuming the substrate. The way that substrate consumption is modeled, however, differs among current SOM models [*Manzoni and Porporato*, 2009]. The most commonly used approach (as in CENTURY) is a linear function, in which the decomposition rate is expressed as simple first-order kinetics with substrate (Figure 1a). This approach postulates that decomposition is a donor-controlled process, implicitly assuming that microbes respond so rapidly to changes in substrate availability that their biomass never limits the decomposition rates. The decomposition rate of this linear model, $DEC_{i,\mathrm{LIN}}$ (g C kg^{-1} soil day^{-1}), equals:

$$DEC_{i,\mathrm{LIN}} = k_{i,\mathrm{LIN}} \cdot C_i \tag{1}$$

where i is the substrate pool (i = S1 [easily decomposable substrate] or i = S2 [recalcitrant substrate]), C_i is the carbon concentration of substrate i (g C kg^{-1} soil), and $k_{i,\mathrm{LIN}}$ is the decomposition coefficient of C_i (day^{-1}). Here, $k_{i,\mathrm{LIN}}$ is described according to CENTURY, and it is modified by soil temperature, moisture, and texture (Appendix A).

Another approach of decomposition takes limitations by microbes into consideration (Figure 1b), and decomposition is assumed to increase linearly with concentrations of both microbes and substrates [e.g., *Porporato et al*., 2003]. The decomposition rate of this multiplicative model, $DEC_{i,\mathrm{MUL}}$ (g C kg^{-1} soil day^{-1}), equals:

$$DEC_{i,\mathrm{MUL}} = k_{i,\mathrm{MUL}} \cdot C_i \cdot C_\mathrm{B} \tag{2}$$

where $k_{i,\mathrm{MUL}}$ is the decomposition coefficient of C_i (day^{-1}) and C_B is the microbial biomass (g C kg^{-1} soil). We estimated the value of $k_{i,\mathrm{MUL}}$ such that equation (1) equals equation (2) when C_B is the median value of a global study ($C_{\mathrm{B\_gl}}$ = 0.87 g C kg^{-1} soil [*Cleveland and Liptzin*, 2007]): $k_{i,\mathrm{MUL}} = k_{i,\mathrm{LIN}} / C_{\mathrm{B\_gl}}$.

Alternatively, decomposition can be formulated as an enzyme-catalyzed reaction (Figure 1c). Decomposition depends on the enzymes produced by microbes as well as on substrate concentration [e.g., *Allison et al*., 2010; *Manzoni and Porporato*, 2007; *Schimel and Weintraub*, 2003]. Assuming that enzyme production is proportional to microbial biomass, the decomposition rate, $DEC_{i,\mathrm{MM}}$ (g C kg^{-1} soil day^{-1}), can be formulated with a simple Michaelis-Menten kinetics:

$$DEC_{i,\mathrm{MM}} = k_{i,\mathrm{MM}} \cdot \frac{C_i}{km_i + C_i} \cdot C_\mathrm{B} \tag{3}$$

where $k_{i,\mathrm{MM}}$ is the decomposition coefficient of C_i (day^{-1}) and km_i is the half saturation constant of C_i (g C kg^{-1} soil). We took the km_i values from *Allison et al*. [2010] assuming a soil temperature of 20°C and a bulk density of 1 g/cm^3: km_{S1} = 0.3 and km_{S2} = 600 g C kg^{-1} soil. We estimated the value of $k_{i,\mathrm{MM}}$ such that equation (1) equals equation (3) at global median values of microbial biomass and soil total C ($C_{\mathrm{TOT\_gl}}$ = 46 g C kg^{-1} soil [*Cleveland and Liptzin*, 2007]) with additional assumptions of $C_\mathrm{B} = 0.5 \cdot C_{\mathrm{S1}}$ and $C_{\mathrm{S2}} \approx C_{\mathrm{TOT}}$: $k_{\mathrm{S1,MM}} = k_{\mathrm{S1,LIN}} \cdot (km_{\mathrm{S1}} + 2 \cdot C_{\mathrm{B\_gl}}) / C_{\mathrm{B\_gl}}$, and $k_{\mathrm{S2,MM}} = k_{\mathrm{S2,LIN}} \cdot (km_{\mathrm{S2}} + C_{\mathrm{TOT\_gl}}) / C_{\mathrm{B\_gl}}$.

Soil respiration rates can be calculated for each type of microbial substrate consumption kinetics as:

$$potCmin_c = \sum_{i=\mathrm{S1}}^{\mathrm{S2}} (1 - e_i) \cdot DEC_{i,c} \tag{4}$$

Table 1. Model Variables and Parameters

Symbol	Unit	Description
Variables (continuous)		
C_B	g C kg^{-1} soil	Microbial biomass
C_{B_gl}	g C kg^{-1} soil	Median value of C_B in a global study
C_i	g C kg^{-1} soil	Carbon concentration in substrate *i*
C_{TOT}	g C kg^{-1} soil	Soil total C
C_{TOT_gl}	g C kg^{-1} soil	Median values of C_{TOT} in a global study
$Cmin_{m,c}$	g C kg^{-1} soil day^{-1}	Actual soil respiration rates, with substrate consumption kinetics *c* and with C:N stoichiometry effect *m*
$DEC_{i,c}$	g C kg^{-1} soil day^{-1}	Decomposition rate of substrate *i* with substrate consumption kinetics *c*
e_i	Fraction between 0 and 1	Microbial growth efficiency when assimilating substrate *i*
$e_{i,m}$	Fraction between 0 and 1	Microbial growth efficiency when assimilating substrate *i*, with C:N stoichiometry effect *m*
imm_max	g N kg^{-1} soil day^{-1}	Maximum N immobilization rate
$k_{i,c}$	day^{-1}	Decomposition coefficient of C_i with substrate consumption kinetics *c*
km_i	g C kg^{-1} soil	Half saturation constant of C_i
$I_{m,c}$	Fraction between 0 and 1	Inhibition factor on decomposition, with substrate consumption kinetics *c* and with C:N stoichiometry effect *m*
N_i	g N kg^{-1} soil	Nitrogen concentration in substrate *i*
NC_B	–	N:C ratio of microbes
NC_i	–	N:C ratio of substrate *i*
$Nmin_{m,c}$	g N kg^{-1} soil day^{-1}	Actual N mineralization rates, with substrate consumption kinetics *c* and with C:N stoichiometry effect *m*
$O_{m,c}$	g C kg^{-1} soil day^{-1}	Overflow of C at low N, with substrate consumption kinetics *c* and with C:N stoichiometry effect *m*
$potCmin_c$	g C kg^{-1} soil day^{-1}	Potential soil respiration rates with substrate consumption kinetics *c* (when N is not limiting decomposition processes)
$potNmin_c$	g N kg^{-1} soil day^{-1}	Potential N mineralization rate with substrate consumption kinetics *c*
Variables (category)		
c		Substrate consumption kinetics (*c* = LIN, MM, or MUL)
i		Substrate pool (*i* = S1 or S2)
m		Microbial C:N stoichiometry effect (*m* = none, INHin, INHorg, COin, or COorg)
Category labels		
LIN		Linear consumption kinetics
MUL		Multiplicative consumption kinetics
MM		Michaelis-Menten consumption kinetics
S1		Easily decomposable substrate
S2		Recalcitrant substrate
none		No C:N stoichiometry effect
INHin		Inhibition effects of N limitation on decomposition triggered by inorganic N
INHorg		Inhibition effect of N limitation on decomposition triggered by organic N
COin		C overflow upon N limitation triggered by inorganic N
COorg		C overflow upon N limitation triggered by organic N

where $potCmin_c$ (g C kg^{-1} soil day^{-1}) is the soil respiration rate calculated with microbial substrate consumption kinetics *c* (*c* = LIN, MUL, or MM) and e_i (fraction between 0 and 1) is the growth efficiency of microbes when assimilating substrate *i*. Note that $potCmin_c$ is the potential decomposition rate when C, but not N, is limiting decomposition processes. The actual soil respiration rates can deviate from the potential decomposition rates when N is limiting (see the following section).

N mineralization is coupled strongly to the decomposition of C, as both N and C are bound to organic compounds. When soil N is not limiting, the rate of N mineralization (i.e., potential N mineralization rate $potNmin_c$, g N kg^{-1} soil day^{-1}) depends solely on the amount of C decomposed and the C:N ratios of microbes

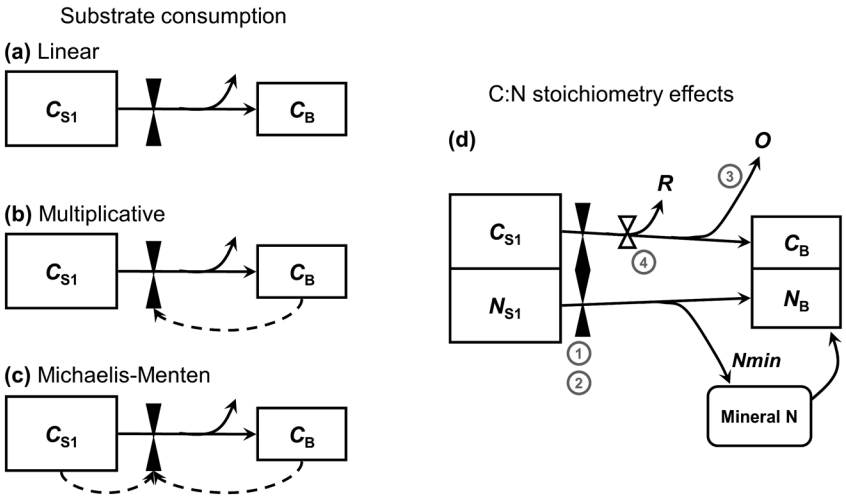

Figure 1. Model structure of C and N in microbes (C_B and N_B) and in easily decomposable substrate pool (C_{S1} and N_{S1}). The interactions between microbes and recalcitrant substrate pool (C_{S2} and N_{S2}) are not shown but identical to C_B-C_{S1} and N_B-N_{S1} interactions. Solid lines represent flows of C and N, whereas dashed lines represent influence on flow rates. (a–c) Three approaches of substrate consumption by microbes: linear (LIN), multiplicative (MUL), and Michaelis-Menten (MM). (d) Four mechanisms of microbial C:N stoichiometry effects on C flows: 1. inhibition effect triggered by inorganic N (INHin); 2. inhibition effect triggered by organic N (INHorg); 3. C overflow triggered by inorganic N (COin); and 4. C overflow triggered by organic N (COorg). INHin and INHorg influence decomposition rates, COin affects C overflow which is not related to microbial growth (*O*), and COorg influences microbial growth efficiency. *R* represents growth-related respiration, and *Nmin* represents N mineralization.

and substrate. When assuming that all available organic N is assimilated by microbes prior to mineralization to ammonium, $potNmin_c$ can be formulated as the difference between N released from the decomposed organic compounds and N assimilated into microbial biomass as [*Manzoni and Porporato*, 2009]:

$$potNmin_c = \sum_{i=S1}^{S2} \left(DEC_{i,c} \cdot NC_i - DEC_{i,c} \cdot e_i \cdot NC_B \right) \tag{5}$$

where NC_i is the N:C ratio of substrate i and NC_B is the N:C ratio of microbes. This is the same approach as in the original version of CENTURY (although later versions allow varying N:C ratio of receiving pools depending on soil mineral N concentrations [*Metherell et al*., 1993; *Parton et al*., 1993]: see *Manzoni and Porporato* [2009] for the possible consequences of relaxing the constant N:C ratio on decomposition). Negative values of $potNmin_c$ mean net N immobilization, instead of N mineralization.

In N-poor conditions, microbial activities can be limited by N rather than C, because microbes are stoichiometrically constrained. The hypothetical mechanisms behind the microbial C:N stoichiometry effects on C and N fluxes (denoted as m, explained in detail later) are diverse across SOM models. Independent of the approach, however, actual soil respiration rates, $Cmin_{m,c}$ (g C kg^{-1} soil day^{-1}), and actual N mineralization rates, $Nmin_{m,c}$ (g N kg^{-1} soil day^{-1}), can be expressed as:

$$Cmin_{m,c} = \sum_{i=S1}^{S2} \left(1 - e_{i,m}\right) \cdot I_{m,c} \cdot DEC_{i,c} + O_{m,c} \tag{6}$$

$$Nmin_{m,c} = \sum_{i=S1}^{S2} \left(I_{m,c} \cdot DEC_{i,c} \cdot NC_i - I_{m,c} \cdot DEC_{i,c} \cdot e_{i,m} \cdot NC_B \right) \tag{7}$$

where $e_{i,m}$ is the microbial growth efficiency when assimilating substrate i, $I_{m,c}$ is an inhibition factor on decomposition (ranging from 0 for full to 1 for no inhibition), and $O_{m,c}$ is an overflow of C at low N (g C kg^{-1} soil day^{-1}) (these variables are explained in detail below) for the microbial substrate consumption kinetics c. When N is not limiting (m = none), the parameter values are set as: $e_{i,\mathrm{none}} = 0.45$ (as in CENTURY); $I_{\mathrm{none},c} = 1$ (no reduction in decomposition); and $O_{\mathrm{none},c} = 0$ (no C overflow). This leads to $Cmin_{\mathrm{none},c} = potCmin_c$ and $Nmin_{\mathrm{none},c} = potNmin_c$. Below, we identify four contrasting types of C:N stoichiometry effects on soil respiration and N mineralization (m = INHin, INHorg, COin, or COorg; see Table 2 and Figure 1d for an overview).

Table 2. Different Assumptions of C:N Stoichiometry Effects (m) Employed in the Model[a]

	m =				
	INHin	INHorg	COin	COorg	None
$I_{m,c}$	Equation ((8))	Equation ((9))	1	1	1
$e_{i,m}$	0.45	0.45	0.45	Equation ((11))	0.45
$O_{m,c}$	0	0	Equation ((10))	0	0

[a]See equations (6) and (7) for how soil respiration and N mineralization rates are affected by $I_{m,c}$, $e_{i,m}$, and $O_{m,c}$. Note that $I_{m,c}$, $e_{i,m}$, and $O_{m,c}$ depend on substrate i (i = S1 or S2) and/or the choice of microbial substrate consumption kinetics c (c = LIN, MM, or MUL).

Most commonly (including later versions of CENTURY), the decomposition rate at N-limited conditions is reduced to the point that inorganic N in soil can provide enough N for the microbial needs (the "INHin" mechanism, affecting the decomposition process (1) in Figure 1d). The inhibition factor $I_{\mathrm{INHin},c}$ can be formulated as [*Manzoni and Porporato*, 2007; *Porporato et al*., 2003]:

$$I_{\mathrm{INHin},c} = \begin{cases} 1 & potNmin_c \geq imm\_max \\ \dfrac{imm\_max}{potNmin_c} & potNmin_c < imm\_max \end{cases} \tag{8}$$

where imm_max is the maximum N immobilization rate (g N kg^{-1} soil day^{-1}), which is by definition a negative value. imm_max can be a function of soil inorganic N or of microbial biomass. Here, we arbitrarily chose a value of -0.0002 g N kg^{-1} soil day^{-1}.

Alternatively, it is proposed that the inhibition effect of N limitation is directly triggered by organic N (the "INHorg" mechanism, affecting the decomposition process (2) in Figure 1d), rather than inorganic N. Here, organic N inhibits decomposition as soon as N demand of microbes according to C decomposition (i.e., $DEC_{i,c} \cdot e_{i,m} \cdot NC_{\mathrm{B}}$) is larger than N assimilated from organic N (i.e., $DEC_{i,c} \cdot NC_i$). The inhibition factor $I_{\mathrm{INHorg},c}$ is formulated as [*Manzoni and Porporato*, 2009]:

$$I_{\mathrm{INHorg},c} = \begin{cases} 1 & potNmi_{nc} \geq 0 \\ \dfrac{\sum_{i=\mathrm{S1}}^{\mathrm{S2}} DEC_{i,c} \cdot NC_{\mathrm{i}}}{\sum_{i=\mathrm{S1}}^{\mathrm{S2}} DEC_{i,c} \cdot e_{i,\mathrm{INHorg}} \cdot NC_{\mathrm{B}}} & potNmin_c < 0 \end{cases} \tag{9}$$

Another possible mechanism of C:N stoichiometry effects is that, when N is limited, excess C is released as waste through an overflow metabolism (the "COin" mechanism, affecting the respiration not related to microbial growth (3) in Figure 1d) [*Schimel and Weintraub*, 2003], instead of inhibiting decomposition. The overflow of C, $O_{\mathrm{COin},c}$ (g C kg^{-1} soil day^{-1}), can be formulated as the difference between assimilated C and C fixed in microbial biomass using total incoming N (i.e., mineralized N from organic sources and immobilized N from inorganic sources):

$$O_{\mathrm{COin},c} = \begin{cases} 0 & potNmin_c \geq imm\_max \\ \sum_{i=\mathrm{S1}}^{\mathrm{S2}} DEC_{i,c}\left(e_{i,\mathrm{COin}} - \dfrac{NC_i}{NC_{\mathrm{B}}}\right) - \dfrac{imm\_max}{NC_{\mathrm{B}}} & potNmin_c < imm\_max \end{cases} \tag{10}$$

Note that this model does not have any impact on N mineralization rates but only on C mineralization.

C overflow may also occur in response to organic N limitation (the "COorg" mechanism, affecting the C overflow process (4) in Figure 1d). In that case, it is assumed that microbes decrease their growth efficiency to use C when the organic substrate is N poor. Thus, unlike with the COin mechanism which has a threshold value of N availability to trigger extra C outflow, C outflow increases gradually as the substrate becomes N poor. Based on a global analysis of litter decomposition, an empirical relationship was derived as [*Manzoni et al*., 2008]:

$$e_{i,\mathrm{COorg}} = 0.43 \cdot \left(\frac{NC_i}{NC_{\mathrm{B}}}\right)^{0.6} \tag{11}$$

Note that equation (11) describes only one possible mechanism through which MGE is influenced. Other factors include temperature, moisture, and substrate quality [*Manzoni et al*., 2012]. Provided that NC_i partly reflects substrate quality, equation (11) can be more broadly interpreted as an integrative description of

substrate quality effects on MGE. Most existing models (including CENTURY) use constant MGE values [*Manzoni et al.*, 2012], whereas the sensitivity of MGE to C and N fluxes has rarely been tested [but see *Allison et al.*, 2010; *Frey et al.*, 2013]. Therefore, this study also intends to examine the effect of adaptive MGE (to substrate N richness) on model behavior.

2.2. Model Sensitivity Analysis

We tested the sensitivity of modeled *Cmin* and *Nmin* to different model settings. The sensitivity was tested within the typical ranges of the parameter values in a surface soil layer as derived from global studies [*Cleveland and Liptzin*, 2007; *Manzoni et al.*, 2008; *Six et al.*, 2006] in terms of relative rates per unit soil C ($Cmin/C_{TOT}$ and $Nmin/C_{TOT}$), rather than *Cmin* and *Nmin*, in order to standardize the model outputs. When not specified, we assumed: $e_{i,m} = 0.45$ (value in CENTURY); $C_B/C_{TOT} = 0.023$ and $C_{TOT} = 46$ (global median values); $C_{S1} = 2 \cdot C_B$; $C_{S2} = C_{TOT}\text{-}C_{S1}\text{-}C_B$; $NC_{S1} = NC_{S2}$ = (soil total N):(soil total C); 50% sand content; 5% clay content; soil temperature 20°C; and no reduction effect by soil moisture.

First, for each type of microbial substrate consumption kinetics (LIN/MM/MUL), relative respiration ($Cmin/C_{TOT}$) was compared to the global ranges of soil total C (C_{TOT}), microbial fraction (C_B/C_{TOT}), and microbial growth efficiency ($e_{i,m}$). Here, no C:N stoichiometry effects were assumed. Second, for each type of C:N stoichiometry effect (INHin/INHorg/COin/COorg/none), relative respiration ($Cmin/C_{TOT}$) and relative N mineralization ($Nmin/C_{TOT}$) were compared to the global range of substrate N:C ratio (NC_i), with three levels of microbial N:C ratio (NC_B). Here, the LIN model was used.

2.3. Model Validation Data Set

We collected top soils from 36 sites in the Netherlands, covering a wide range of nutrient, acidity, and moisture conditions [*Fujita et al.*, 2013], in order to determine soil physical and chemical variables, microbial biomass and stoichiometry, and C and N fluxes in soil incubation experiments. In addition, we retrieved published data with a similar set of soil information from temperate and boreal ecosystems (Table 3). This led to 154 sites for *Cmin* and 45 sites for *Nmin*.

Microbial C was estimated with either the chloroform fumigation-extraction method or the substrate-induced respiration method. See Appendix B for justification to treat the estimates of both methods as being equivalent. *Cmin* was measured for incubation periods of 2 h to 1 day, with a few exceptions of 10 days (five sites). Soil moisture condition was in most cases adjusted to be "optimal" (i.e., respiration not hampered by either oxygen or water stress), and temperature was adjusted to 20–25°C. See Table 3 for methodological details of each study. *Nmin* was measured at the same conditions as *Cmin* but for longer periods (6 weeks to 1 month). For one data set in which soil moisture was adjusted to the highest level (db1 in Table 3, WFPS 80%), measured N mineralization rates were corrected for N loss by adding denitrification rates predicted with DAYCENT model equations [*Del Grosso et al.*, 2002] (for details, see *Fujita et al.* [2013]). For the majority of the sites, the predicted denitrification rates were small. For 13 out of the 36 sites, however, the modeled denitrification rate was rather large (i.e., >0.1 mg N kg^{-1} soil day^{-1} and $>10\%$ of the measured N mineralization rate).

Table 3. Details of the Data Sets of Soil Incubation Experiments Used for Model Validation

				Pool Size Estimate Method			Incubation Experiment						
No.[a]	Country	N	Soil Depth	Soil Texture	Soil Total C/N[b]	Microbial Measure[c] (element)	Temp	Moisture	Duration *Cmin*	Method[d] *Cmin*	Duration *Nmin*	Extraction Method *Nmin*
db1	Netherlands	36	0–15 cm	sand/silt/clay	CN[e]/CN	FE (C,N)	20°C	80% WFPS	2 h	GC	42 days	1 M KCl
db2	New Zealand	3	0–10 cm	NA[f]	CO/KJ	FE (C,N)	25°C	60% WFPS	10 days	KOH	56 days	2 M KCl
db3	New Zealand	2	0–10 cm	NA[f]	CO/KJ	FE (C,N)	25°C	60% WFPS	10 days	KOH	56 days	2 M KCl
											1 month/	
db4	Luxembourg	4	0–5 cm	NA[f]	CN/CN	FE (C,N)	20°C	"optimal"[g]	1 day	GC	42 days	0.5 M K_2SO_4
db5	Germany	4	0–10 cm	NA	CO[e]/CO	SIR (C)	22°C	−240 kPa	10 h	GC	–	–
db6	Germany (European)	88	0–15 cm	sand[h]	CN[e]/CN	SIR (C)	20°C	As in field 50–60%	8–18 h	GC	–	–
db7	Russia	17	0–10 cm	sand/silt/clay	DI/KJ	SIR (C)	22°C	WFPS	1 day	GC	–	–

WFPS: water filled pore space (fraction between 0 and 1); *Cmin*: soil respiration rates; *Nmin*: soil N mineralization rates.
[a]References are db1: this study; db2: *Ross et al.* [1999]; db3: *Ross et al.* [1996]; db4: *Kooijman et al.* [2008]; db5: *Blagodatskaya and Anderson* [1998]; db6: *Wirth* [2001]; and db7: *Ananyeva et al.* [2008].
[b]CN: CN analyzer, CO: combustion, DI: dichromate digestion, KJ: Kjeldahl digestion.
[c]FE: chloroform fumigation-extraction method, SIR: substrate-induced respiration method with added glucose (see Appendix B for conversion factors).
[d]GC: Gas chromatography, KOH: adsorbed in 0.1 M KOH and estimated by titration of excess alkali with 50 mM HCl after precipitation of K_2CO_3 by 1 M $BaCl_2$.
[e]Amount of inorganic C was subtracted to estimate organic C only.
[f]Texture was estimated based on the textural class, according to soil texture triangle of USDA.
[g]Gravimetric moisture content was 300% for organic and 50% for mineral soil samples.
[h]Clay content was approximated as 22% (average value of db1 and db7) of non-sand content.

2.4. Validating Soil Respiration and N Mineralization Rates

Prior to our validation, we determined the relationship between soil texture and respiration rates. Contrary to the assumption of CENTURY model that *Cmin*, expressed as a ratio to soil total C, is negatively related to the clay plus silt content, they were positively related in our validation data set (see Appendix C for more details). To avoid texture adversely affecting the modeled relations, we employed an arbitrarily chosen fixed value of sand and clay content (50% and 5%, respectively) for all sites.

We compared measured and predicted *Cmin* to test model performance for the different approaches of substrate consumption (LIN/MUL/MM) and C:N stoichiometry (INHin/INHorg/COin/COorg), and for different site-specific input values of microbial properties (constant/measured) (see Table 4 for an overview). First, for each approach of substrate consumption, we predicted *Cmin* with no site-specific microbial information (i.e., site-specific input values are soil total C and incubation temperature only) and no C:N stoichiometry effects. Here, the microbial fraction (C_B/C_{TOT}, where $C_{TOT} = C_B + C_{S1} + C_{S2}$) was set to 1% according to the initial value of CENTURY [*Metherell et al*., 1993]. Second, the constant microbial fraction was replaced with the measured microbial fraction. Third, we tested the four different approaches of the C:N stoichiometry effect (INHin/INHorg/COin/COorg) with measured microbial fraction. A constant microbial N:C ratio (NC_B) (0.14, the median value of a global data set [*Cleveland and Liptzin*, 2007]) was applied, and soil N pools were initiated such that the N:C ratio of the easily decomposable pool (NC_{S1}) is higher than that of the recalcitrant pool (NC_{S2}) (NC_{S1}: NC_{S2} equaling 11:8, as in CENTURY). In addition, for the subset for which NC_B had been measured (45 sites), the constant NC_B was replaced with measured NC_B values. Note that *Cmin* is affected by N:C ratios of substrates and microbes only when C:N stoichiometry effects are included. For all simulations, C_{S1} was assumed to be as twice large as C_B, and we assumed no reduction in decomposition due to soil moisture.

Subsequently, we tested model performance for *Nmin*. *Nmin* was predicted in the same way as for *Cmin* but with LIN model only (since model predictive ability for *Cmin* was better with LIN than with MUL or MM; see section 3). Validation was run with a constant NC_B (0.14) and with the site-specific measured NC_B value. See Table 4 for an overview.

Goodness of fit between observed and predicted *Cmin* and *Nmin* was quantified with Spearman's rank correlation coefficients (ρ) and normalized root mean square error (*nRMSE*). The latter quantifies the "average distance" of observed and predicted values in units of the observation range:

$$nRMSE = 100 \cdot \frac{\sqrt{\sum_{s=1}^{n} (obs_s - pre_s)^2 / n}}{obs_{max} - obs_{min}} \tag{12}$$

where obs_s is the log-transformed observed *Cmin* or *Nmin* of site *s*, pre_s is the log-transformed predicted *Cmin* or *Nmin* of site *s*, *n* is the number of sites, and obs_{max} and obs_{min} are the maximum and minimum values, respectively, of observed log-transformed *Cmin* or *Nmin*.

To evaluate model performance across models with different assumptions, median values and 95% confidence intervals of ρ and *nRMSE* were calculated from 1000-time bootstrapped sites (154 sites for *Cmin* and 45 sites for *Nmin*) [*Good*, 2005]. If fewer than 5% of the computed ρ or *nRMSE* for a model exceeded the median value of another model, we considered the change in the model predictive ability as significant ($P < 0.05$).

3. Results

3.1. Sensitivity of Modeled Soil Respiration to Microbial Substrate Consumption, Microbial Biomass, and Microbial Growth Efficiency

Figure 2 shows the sensitivities of modeled relative respiration rate, $Cmin/C_{TOT}$, for each type of substrate consumption kinetics given the 5th to 95th percentile of soil total C (C_{TOT}), microbial fraction (C_B/C_{TOT}), and MGE ($e_{i,m}$) from global studies. The patterns of relative respiration were contrasting among LIN, MUL, and MM models. With the LIN model, relative respiration was constant for all levels of C_{TOT} (Figure 2a), whereas relative respiration increased with increasing C_{TOT} with the MUL and MM models (Figures 2b and 2c, respectively). The sensitivity of relative respiration to C_{TOT} was stronger in the MUL model than in the MM model: relative respiration increased 19.3× with the MUL model and 2.9× with the MM model when C_{TOT}

Table 4. Overview of Model Assumptions to Predict Soil Respiration and N Mineralization Rates of the Validation Data Set and Their Goodness-of-Fit (in Normalized Root Mean Square Errors *nRMSE* and Spearman's Rank Correlation Coefficients ρ) With Observed Data

	Model Assumptions					Model Fit	
ID	Substrate Consumption (*c*)	Microbial Fraction (C_B/C_{TOT})	C:N Stoichiometry (*m*)	Microbial N:C ratio (NC_B)	Fig No.[a]	*nRMSE* (%)	ρ
			Soil Respiration				
LIN	LIN	1%[c]	none	–	S5a	45.4	0.66***
LIN_Cb	LIN	measured	none	–	S5b	21.3	0.78***
LIN_Cb_INHin	LIN	measured	INHin	0.14[d]	S5c	56.4	0.57***
LIN_Cb_INHorg	LIN	measured	INHorg	0.14	S5d	21.6	0.78***
LIN_Cb_COin	LIN	measured	COin	0.14	S5e	21.3	0.79***
LIN_Cb_COorg	LIN	measured	COorg	0.14	S5f	19.5	0.76***
MUL	MUL	1%	none	–	S5g	95.7	0.65***
MUL _Cb	MUL	measured	none	–	S5h	41.2	0.78***
MUL _Cb_INHin	MUL	measured	INHin	0.14	S5i	66.3	0.56***
MUL _Cb_INHorg	MUL	measured	INHorg	0.14	S5j	41.3	0.78***
MUL _Cb_COin	MUL	measured	COin	0.14	S5k	41.6	0.78***
MUL _Cb_COorg	MUL	measured	COorg	0.14	S5l	39.5	0.77***
MM	MM	1%	none	–	S5m	71.9	0.65***
MM _Cb	MM	measured	none	–	S5n	27.6	0.79***
MM _Cb_INHin	MM	measured	INHin	0.14	S5o	60.3	0.52***
MM _Cb_INHorg	MM	measured	INHorg	0.14	S5p	27.8	0.78***
MM _Cb_COin	MM	measured	COin	0.14	S5q	27.6	0.79***
MM _Cb_COorg	MM	measured	COorg	0.14	S5r	25.9	0.78***
			N Mineralization				
N	LIN	1%	none	0.14	S8a	29.0	ns
N_Cb	LIN	measured	none	0.14	S8b	31.0	ns
N_INHin	LIN	measured	INHin	0.14	S8c	27.6	ns
N_INHorg	LIN	measured	INHorg	0.14	S8d	31.0	ns
N_COin[b]	LIN	measured	COin	0.14	S8e	31.0	ns
N_COorg	LIN	measured	COorg	0.14	S8f	25.3	0.41**
N_nc	LIN	1%	none	measured	S8g	29.6	ns
N_Cb_nc	LIN	measured	none	measured	S8h	35.8	ns
N_INHin_nc	LIN	measured	INHin	measured	S8i	32.9	ns
N_INHorg_nc	LIN	measured	INHorg	measured	S8j	35.8	ns
N_COin_nc[b]	LIN	measured	COin	measured	S8k	35.8	ns
N_COorg_nc	LIN	measured	COorg	measured	S8l	22.2	0.35*

ns: not significant ($P > 0.05$);
*$P < 0.05$;
**$P < 0.01$;
***$P < 0.001$.
[a]Figure numbers corresponding to those in Figure S5 in Appendix D and Figure S8 in Appendix G.
[b]This assumption of N limitation does not affect N mineralization rates (but does affect respiration rates).
[c]Initial value of CENTURY [*Metherell et al.*, 1993].
[d]The median value of global data set [*Cleveland and Liptzin*, 2007].

increased from the 5th to the 95th percentile of its global values. Note that the sensitivity of the MM model changed with the choice of the half-saturation parameter values (km_{S1} and km_{S2}): the sensitivity of relative respiration increased to 3.8× when km_i values were doubled, whereas it decreased to 2.3× when km_i values were halved.

The effect of microbial biomass on relative respiration was strong, especially for the MUL model. Within the global 5th–95th percentile of microbial fraction (i.e., a 12.6× difference), relative respiration increased 6.5× for the LIN model (Figure 2d), 82.2× for the MUL model (Figure 2e), and 15.6× for the MM model (Figure 2f) when C_{TOT} was the global median value. The MUL model led to an unrealistic relative respiration (i.e., higher than its global range) whenever microbial fraction and C_{TOT} exceeded its global 75th percentile values (Figures 2b and 2e).

From the 5th to 95th percentile of the global MGE values (i.e., a 20.7× increase), relative respiration declined about 3× irrespective of the substrate consumption kinetics and C_{TOT} (Figures 2g–2i).

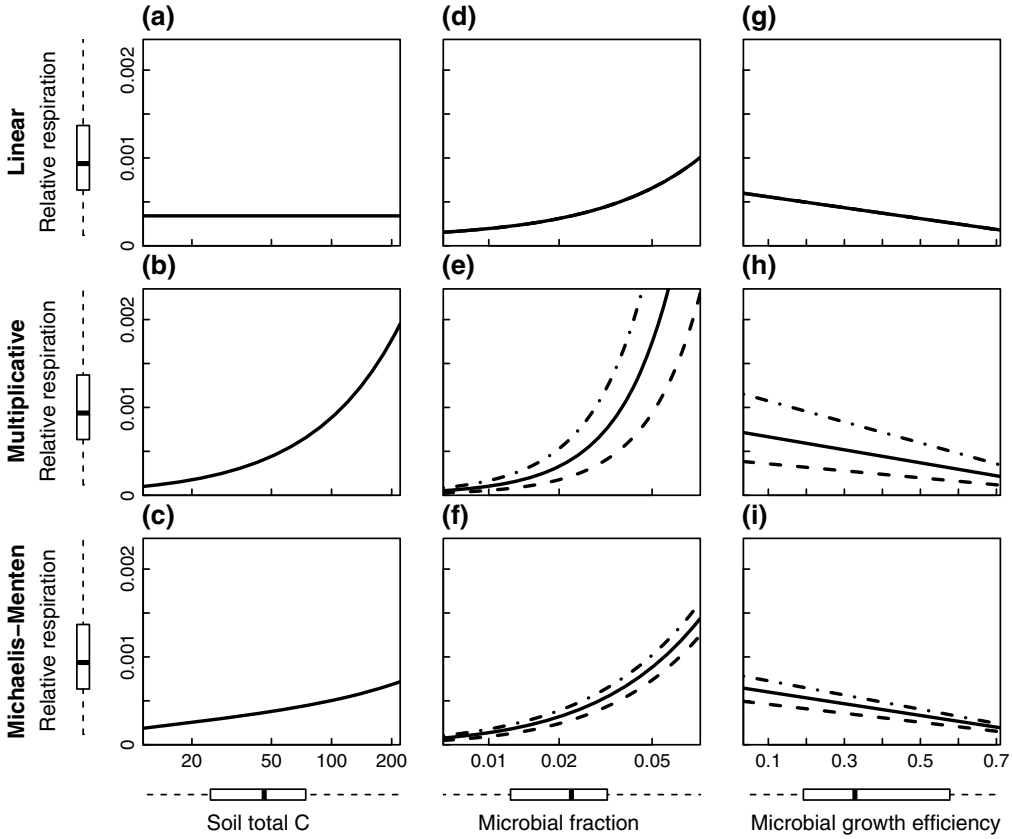

Figure 2. Sensitivity of relative respiration rate ($Cmin/C_{TOT}$, day^{-1}) to soil total C (C_{TOT}, g C kg^{-1} soil), microbial fraction (C_B/C_{TOT}), and microbial growth efficiency ($e_{i,m}$) for three model approaches of substrate consumption (a,d,g: linear (LIN), b,e,h: multiplicative (MUL), c,f,i: Michaelis-Menten (MM)). For the multiplicative and Michaelis-Menten models, the model behavior against microbial fraction and microbial growth efficiency depends on soil total C. Soil total C values were 24.8 (dashed line), 46.0 (solid line), and 74.3 (dot-dash-line), representing the 25th, 50th, and 75th percentiles of a global data set [*Cleveland and Liptzin*, 2007, $N = 155$]. Box plots show the 25th, 50th, and 75th percentiles of the global data set of soil total C and microbial fraction [*Cleveland and Liptzin*, 2007, $N = 144$], microbial growth efficiency (measured with mixed microbial community for litter [*Manzoni et al.*, 2008] and soil [*Six et al.*, 2006], $N = 112$), and relative respiration (this study, $N = 154$), with whiskers extending to the 5th and 95th percentiles. We assumed $C_B/C_{TOT} = 0.023$ for Figures 2a–2c and 2g–2i, and $e_{i,m} = 0.45$ for Figures 2a–2f.

3.2. Sensitivity of Soil Respiration and N Mineralization to Microbial C:N Stoichiometry Effects

Different approaches to modeling C:N stoichiometry effects led to opposing patterns of soil respiration for N-poor to N-rich conditions (Figures 3a–3c). When an inhibiting effect on decomposition was assumed (INHin and INHorg), relative respiration decreased with decreasing substrate N:C ratio (NC_i, for which $NC_{S1} = NC_{S2}$ was assumed) from a threshold value of NC_i onward (grey lines in Figures 3a–3c). In contrast, when N limitation was assumed to occur through an overflow of C (COin and COorg), relative respiration increased with decreasing NC_i (black lines in Figures 3a–3c). In both cases, when inorganic N triggered the effect (INHin and COin; dotted lines in Figures 3a–3c), the threshold values of NC_i where N limitation starts were lower, but the magnitude of change in relative respiration following the threshold was larger.

A higher microbial N:C ratio, NC_B, amplified the C:N stoichiometry effects on relative respiration (from Figures 3a to 3c), as the increasing demand of microbes for N increased the threshold value of NC_i, and therefore N limitation occurred at a less N-poor substrate.

The choice of the C:N stoichiometry effect had a less striking, but still substantial, effect on N mineralization (Figures 3d–3f). If there was no C:N stoichiometry effect (thick lines in Figures 3d–3f), relative N mineralization rates (i.e., $Nmin/C_{TOT}$) decreased with decreasing NC_i because a larger fraction of assimilated N was fixed by microbes and less N was released to the soil. As NC_i decreased further, N was eventually immobilized from

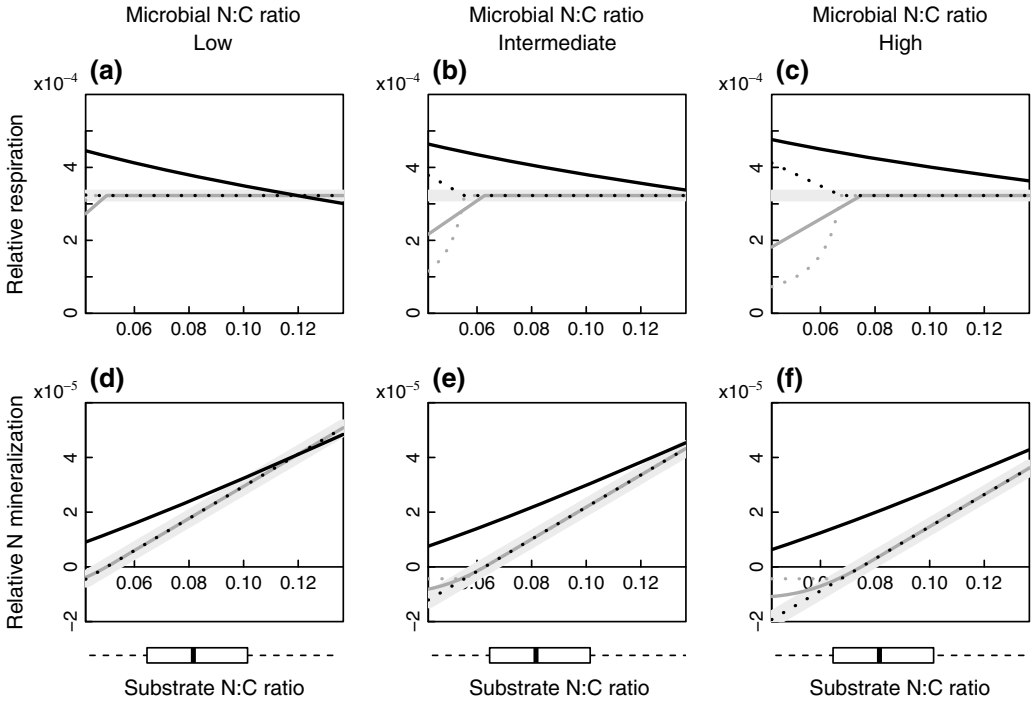

Figure 3. (a–c) Sensitivity of relative respiration rate ($Cmin/C_{TOT}$, day^{-1}) and (d–f) relative N mineralization rate ($Nmin/C_{TOT}$, g N g^{-1} C day^{-1}) against substrate N:C ratio (NC_i), with different approaches of the microbial C:N stoichiometry effects on C fluxes. The microbial C:N stoichiometry effect is described as INHin (dotted grey lines), INHorg (solid grey lines), COin (dotted black lines), and COorg (solid black lines), and no effect of C:N stoichiometry (thick grey lines). Sensitivity is shown for three different levels of microbial N:C ratio (NC_B); ($NC_B = 0.11$, left) low, ($NC_B = 0.14$, middle) intermediate, and ($NC_B = 0.17$, right) high levels, which corresponds to the 25th, 50th, and 75th percentiles of a global data set [*Cleveland and Liptzin*, 2007, $N = 134$]. Box plots show the 25th, 50th, and 75th percentiles of the global data set of NC_i [*Cleveland and Liptzin*, 2007, $N = 145$], with whiskers extending to the 5th and 95th percentiles. We used the linear model (LIN) and assumed $C_{TOT} = 46$, $C_B/C_{TOT} = 0.023$, and $e_{i,m} = 0.45$ (except for COorg, in which $e_{i,m}$ varies as a function of NC_i and NC_B).

inorganic N pools. This pattern still occurred when an inhibition effect of C:N stoichiometry was imposed (INHin and INHorg), but the magnitude of N immobilization was diminished (grey lines in Figures 3d–3f). Model behavior was quite different with COorg: relative N mineralization was less suppressed at lower NC_i, because C use efficiency was reduced by decreasing e, and therefore microbial N demands were kept relatively low at N-poor conditions (black solid lines in Figures 3d–3f).

Increasing NC_B decreased relative N mineralization for all models (from Figures 3d to 3f). However, the effect of increasing NC_B was limited for COorg, because a negative effect of high NC_B on relative N mineralization due to increased microbial demand was mitigated by a positive effect via decreasing MGE.

3.3. Model Validation for Soil Respiration Rates

The LIN model with minimal site-specific input values (soil total C and incubation temperature) predicted the rank order of *Cmin* reasonably well ($\rho = 0.66$) but not the magnitude of *Cmin* (*nRMSE* 45.4%) (Table 4; Figure S5a in Appendix D). Use of site-specific C_B data significantly improved *nRMSE* (21.3%, $P < 0.001$) and rank order ($\rho = 0.78$, $P < 0.01$) (Figure S5b; see Appendix E for the difference in model performance tested by bootstrapping). Including the INHin mechanism made model performance significantly ($P < 0.001$) worse (Figure S5c; $nRMSE = 56.4\%$), whereas there was a trend ($P = 0.089$) for the COorg mechanism to improve model predictions (Figure S5f; $nRMSE = 19.5\%$). Including the other mechanisms of C:N stoichiometry effects (INHorg [Figure S5d] and COin [Figure S5e]) did not make any significant change ($P > 0.10$) in model performance.

The MUL model made predictions of *Cmin* worse for all model settings (Table 4 and Figures S5g–S5l) because of model underestimation for organic-poor soils (bottom left side of the graph) and model overestimation for

organic-rich soils (top right side). The MM model gave slightly worse predictions than the LIN model (Table 4 and Figures S5m–S5r), mainly because of model underestimation for organic-poor soils.

With a subset of the sites for which microbial N data were available (45 sites), we also tested if site-specific NC_B data improved model performance for *Cmin*. No significant ($P > 0.05$) improvement was detected in *nRMSE* nor ρ after inclusion of measured NC_B (Appendix F).

3.4. Model Validation for Soil N Mineralization Rates

When NC_B was assumed to be constant, and when no C:N stoichiometry effect was assumed, model performance for *Nmin* was poor irrespective of whether C_B was kept constant (*nRMSE* = 29.0%, Figure S8a in Appendix G) or measured (*nRMSE* = 31.0%, Figure S8b). The poor performance was partly because many sites were falsely predicted to have net N immobilization. Including the INHin mechanism slightly improved the model performance in terms of *nRMSE* (27.6%, $P < 0.05$, Figure S8c) but not the rank order ($\rho = 0.14$, $P > 0.05$), because overestimation of N immobilization was corrected to some extent. Including the COorg mechanism significantly improved the model fit in terms of both *nRMSE* (25.3%, $P < 0.05$) and rank order ($\rho = 0.41$, $P < 0.001$) (Figure S8f). INHorg and COin did not cause any significant difference in model performance ($P > 0.05$).

When measured NC_B was used instead of constant NC_B (Figures S8g–S8l), model performance on *Nmin* was improved significantly only for COorg mechanism in terms of *nRMSE* (22.2%, $P < 0.05$, Figure S8j), yet the rank order remained unchanged ($\rho = 0.35$, $P > 0.05$).

4. Discussion

4.1. Important Model Elements to Improve Across-Site Predictions of Soil C and N Fluxes

Increasing model complexity potentially leads to improved model performance, yet at the expense of increasing efforts and uncertainty in defining input and parameter values. A challenge is to find an optimal complexity given the specific scope of the model and the availability of data. Our study identified the relative importance of components of model complexity (in terms of model structures on microbial processes and microbial parameters) in order to predict C and N fluxes across sites.

Microbial biomass had by far the strongest influence on predicted *Cmin* (Figures 2d–2f). Significant improvement of model predictive ability on *Cmin* when using site-specific microbial biomass data (Table 4) provides empirical evidence that microbial biomass counts for determining *Cmin*. From a model-structure perspective, the sensitivity of *Cmin* to microbial biomass is explained by the much higher (ca. 67×) decomposition coefficient for easily decomposable carbon (k_{S1}) than for recalcitrant carbon (k_{S2}), accounting for approximately 67% of total decomposition irrespective of the small size of the labile carbon pool (derived from equations in Appendix A, assuming 5% clay content and 45% silt content). Note that, even in the LIN model in which the microbial biomass was not explicitly included, partitioning of soil C pools was controlled by microbial biomass (see assumptions in section 2.2). Thus, the improved model fit by using measured microbial biomass does not per se justify the model structure of microbe-substrate relations or specific parameter values involved in our model but reflects the generic dependency of decomposition rate on the size of SOM fractions [*Ros*, 2012] and, therefore, the uncertainty in model performance due to initial fractionation of SOM in models [*Bruun and Jensen*, 2002; *Foereid et al*., 2012].

In contrast to the strong model sensitivity to microbial biomass, the impacts of different substrate consumption kinetics (LIN/MUL/MM) on predicted *Cmin* were minor, except that the MUL model causes unrealistically high predictions for C-rich soils (Figure 2). This implies that the LIN model is sufficient to describe across-site differences in steady-state *Cmin*. Second-order kinetics of decomposition may become important when predicting the temporal dynamics of C in non-steady conditions [*Treseder et al*., 2012; *Whitmore*, 1996] since dynamically changing microbial biomass could have large feedback effects on C cycling [*Allison et al*., 2010; *Wieder et al*., 2013], but that was not tested in our validation data set.

The assumptions employed for microbial C:N stoichiometry effects matter not only for the prediction of N fluxes but also for the prediction of C fluxes. Whether *Cmin* increases or decreases with increasing substrate N richness depends on the presumed mechanism of how microbes cope with N-limited conditions (i.e., INHin/INHorg/COin/COorg) (Figures 3a–3c). Model validation showed that using COorg resulted in the best model

performance for both *Cmin* and *Nmin*, whereas using INHin led to considerable underestimation in predicted *Cmin* and *Nmin* for N-poor soils (Table 4). In addition, decreasing *Cmin* at N-rich conditions (as in COin and COorg), instead of increasing *Cmin* (as in INHin and INHorg), is in accordance with observed patterns in fertilization experiments [*Butnor et al*., 2003; *Janssens et al*., 2010; but see *Lu et al*., 2011; *Ramirez et al*., 2010]. Strikingly, INHin is used in the majority of the existing SOM models that consider C:N stoichiometry effects [*Manzoni and Porporato*, 2009]. Another implication from the model validation was that the C:N stoichiometry mechanisms triggered by substrate N (INHorg, COorg) performed better than those triggered by mineral N (INHin, COin) when predicting *Cmin* (Table 4). Those substrate-driven mechanisms result in earlier emergence of N-limitation effects as a soil becomes N-poor (see tipping points in Figures 3a–3c). Importantly, SOM models adopting these mechanisms will project more rapid responses of soil C upon changed availability of C relative to N (e.g., CO_2 increase, N deposition) than conventional models (i.e., without C:N stoichiometry effects or with INHin mechanism), possibly leading to a considerable deviation in future predictions of global C cycles.

Interestingly, despite the importance of C:N stoichiometry mechanisms, including site-specific microbial C:N ratios did not clearly improve predictions of *Cmin* and *Nmin* (Appendix F). This is largely explained by the fact that the microbial C:N ratio is well constrained even across biomes [*Cleveland and Liptzin*, 2007]. Also, if there is a feedback mechanism of microbes to correct an imbalance between C and N (e.g., high N demand of N-rich microbes is mitigated by decreased MGE when substrate is relatively N-poor [COorg mechanism]), which is a plausible strategy evolved in N-poor environments, among-site variations of microbial C:N ratio will be masked by these feedbacks. Indeed, although model sensitivity to MGE was relatively minor compared to that to microbial biomass (Figures 2g–2i compared to Figures 2a–2c), our model fit did improve when MGE was assumed to be a function of substrate C:N ratios (COorg mechanism) (Table 4). This impact of variation in MGE on model performance reinforces the need for an explicit description of drivers of MGE in SOM models [*Frey et al*., 2013; *Manzoni et al*., 2012; *Sinsabaugh et al*., 2013].

4.2. The Importance and Challenges of Model Validation

Our study provided one of the first across-site validations of SOM models with various microbial processes for both *Cmin* and *Nmin*. Such across-site validations are a crucial step for evaluating the need for consideration of microbial processes and parameters in global soil models [*McGuire and Treseder*, 2010; *Ostle et al*., 2009; *Rastetter et al*., 2003; *Treseder et al*., 2012; *Wieder et al*., 2013]. When locally measured microbial biomass was imposed on our SOM model, across-site variations in C fluxes were predicted well (Table 4). Thanks to a recently developed global microbial biomass map [*Serna-Chavez et al*., 2013], it is now possible to incorporate microbial biomass also into global SOM models. Still, such estimates are available only for the contemporary climate. Moreover, in order to properly incorporate microbial biomass into global models, evaluation of their robustness to environmental drivers in space and time will remain needed. In addition, how microbial processes (for which we defined alternative descriptions) affect C fluxes at non-steady-state conditions needs to be examined with experimental data and validated in field conditions of multiple ecosystems. This highlights the need to continue our efforts to better understand the mechanisms and drivers of C dynamics, as well as to obtain more appropriate data sets for model parameterization.

Across-site model validation studies are even more critically needed for N compared to C. Soil N cycles are more complex compared to soil C cycles, coinciding with generally poorer model predictions for N than for C efflux [Table 4; also, see, e.g., *Kelly et al*., 2000; *Leirós et al*., 1999]. As a consequence, the current implications of N cycling in global models are highly uncertain. This is particularly problematic given the strong feedbacks of N cycling on CO_2 fluxes [*Thornton et al*., 2007]. Provided the importance of C:N stoichiometry effects, standardized flux and pool size measurements alone are likely to be insufficient to further enhance our understanding. Instead, one should aim at measuring gross rates of each process with, for example, isotopic approaches [*Schimel and Bennett*, 2004], although that is not easily realized in field conditions.

4.3. Implications to Improve Global Models

Our study provides important insights for improving SOM models as a crucial part of global models evaluating terrestrial C (and N) fluxes, such as Dynamic Global Vegetation models embedded in Earth system models. The need for including a mechanistic representation of microbial processes, which has been

discussed before [*Todd-Brown et al*., 2011; *Treseder et al*., 2012], was put forward in our study, yielding several vital indications for the required model complexity as follows.

First, microbial biomass, which differs considerably among sites, has to be better understood on global scales to improve model predictions. The recent progress in global databases of microbial biomass and activity [*Cleveland and Liptzin*, 2007; *Fierer et al*., 2009; *Serna-Chavez et al*., 2013; *Sinsabaugh et al*., 2008] allows for a more realistic initialization of microbial biomass and other microbial parameters for global SOM simulations for the contemporary climate. Such efforts should go hand in hand with efforts to improve model initialization of SOM fractionation in global models [*Pietsch and Hasenauer*, 2006].

Second, including the non-linear kinetics of microbial substrate consumption does not seem necessary to improve the model performance, unless capturing temporal fluctuation of fluxes is of main concern.

Finally, the microbial C:N stoichiometry mechanisms certainly need improved understanding and incorporation in global models. Given the increasing recognition on the importance of N feedbacks in global C models [*Esser et al*., 2011; *Gerber et al*., 2010; *Thornton et al*., 2007], rigorous efforts are needed to empirically test microbial feedbacks on C-N interactions (especially those concerning microbial growth efficiency) and to re-evaluate the approach of C:N stoichiometry effects in global SOM models. Detailed biologically realistic microbial models for small-scale applications may, in this context, allow testing of specific processes, eventually speeding up procedures of identifying and reducing model uncertainty, making SOM models more robust and better suited for global change predictions.

Concluding, our study showed that incorporating microbial processes in a simple SOM model considerably reduced prediction errors in soil C and N fluxes across different soil conditions: the predictive ability was improved from 45.4% to 19.5% *nRMSE* for soil respiration and from 29.0% to 22.2% *nRMSE* for soil N mineralization by including site-specific microbial biomass data and microbial N feedbacks on C via altered microbial growth efficiency. This highlights the need to better incorporate microbial mechanisms into global models. Future studies are needed to better understand spatial patterns and its drivers of microbial biomass based on the emerging global databases of microbes, as well as to re-evaluate the mechanisms of soil C-N interactions mediated by microbes. With such advancements, we envision improved predictions of global C and N fluxes for a current and projected climate.

Acknowledgments

This research was carried out in the framework of CARE project of the Dutch national research program Knowledge for Climate and the joint research program of the Dutch Water Utility sector. We thank Staatsbosbeheer, Veluwe national park, and PWN for the permission to sample soils; R. van Logtestijn, J. van Hal, and J. Weedon for their help in measuring microbial properties; W. Roling and M. Braster for their help in using TOC analyzer; H. Roelofsen and J. Runhaar for field sampling; and two anonymous reviewers for their constructive comments. Original data for the model validation is available as in Supporting Information Table S1.

References

Allison, S. D. (2012), A trait-based approach for modelling microbial litter decomposition, *Ecol. Lett.*, *15*(9), 1058–1070.

Allison, S. D., M. D. Wallenstein, and M. A. Bradford (2010), Soil-carbon response to warming dependent on microbial physiology, *Nat. Geosci.*, *3*(5), 336–340.

Ananyeva, N. D., E. A. Susyan, O. V. Chernova, and S. Wirth (2008), Microbial respiration activities of soils from different climatic regions of European Russia, *Eur. J. Soil Biol.*, *44*(2), 147–157.

Bardgett, R. D., C. Freeman, and N. J. Ostle (2008), Microbial contributions to climate change through carbon cycle feedbacks, *ISME J.*, *2*(8), 805–814.

Blagodatskaya, E. V., and T. H. Anderson (1998), Interactive effects of pH and substrate quality on the fungal-to-bacterial ratio and QCO2 of microbial communities in forest soils, *Soil Biol. Biochem.*, *30*(10-11), 1269–1274.

Blagodatsky, S. A., and O. Richter (1998), Microbial growth in soil and nitrogen turnover: A theoretical model considering the activity state of microorganisms, *Soil Biol. Biochem.*, *30*(13), 1743–1755.

Bruun, S., and L. S. Jensen (2002), Initialisation of the soil organic matter pools of the Daisy model, *Ecol. Model.*, *153*(3), 291–295.

Butnor, J. R., K. H. Johnsen, R. Oren, and G. G. Katul (2003), Reduction of forest floor respiration by fertilization on both carbon dioxide-enriched and reference 17-year-old loblolly pine stands, *Global Change Biol.*, *9*(6), 849–861.

Cleveland, C. C., and D. Liptzin (2007), C:N:P stoichiometry in soil: Is there a "Redfield ratio" for the microbial biomass?, *Biogeochemistry*, *85*(3), 235–252.

Del Grosso, S., D. Ojima, W. Parton, A. Mosier, G. Peterson, and D. Schimel (2002), Simulated effects of dryland cropping intensification on soil organic matter and greenhouse gas exchanges using the DAYCENT ecosystem model, *Environ. Pollut.*, *116*(Suppl. 1), S75–S83.

Esser, G., J. Kattge, and A. Sakalli (2011), Feedback of carbon and nitrogen cycles enhances carbon sequestration in the terrestrial biosphere, *Global Change Biol.*, *17*(2), 819–842.

Falkowski, P. G., T. Fenchel, and E. F. Delong (2008), The microbial engines that drive Earth's biogeochemical cycles, *Science*, *320*(5879), 1034–1039.

Fang, C., P. Smith, J. U. Smith, and J. B. Moncrieff (2005), Incorporating microorganisms as decomposers into models to simulate soil organic matter decomposition, *Geoderma*, *129*(3–4), 139–146.

Fierer, N., M. S. Strickland, D. Liptzin, M. A. Bradford, and C. C. Cleveland (2009), Global patterns in belowground communities, *Ecol. Lett.*, *12*(11), 1238–1249.

Foereid, B., P. H. Bellamy, A. Holden, and G. J. D. Kirk (2012), On the initialization of soil carbon models and its effects on model predictions for England and Wales, *Eur. J. Soil Sci.*, *63*(1), 32–41.

Frey, S. D., J. Lee, J. M. Melillo, and J. Six (2013), The temperature response of soil microbial efficiency and its feedback to climate, *Nat. Clim. Change*, *3*(4), 395–398.

Fujita, Y., P. M. van Bodegom, H. Olde Venterink, H. Runhaar, and J.-P. M. Witte (2013), Towards a proper integration of hydrology in predicting soil nitrogen mineralization rates along natural moisture gradients, *Soil Biol. Biochem.*, *58*, 302–312.
Gerber, S., L. O. Hedin, M. Oppenheimer, S. W. Pacala, and E. Shevliakova (2010), Nitrogen cycling and feedbacks in a global dynamic land model, *Global Biogeochem. Cycles*, *24*, GB1001, doi:10.1029/2008GB003336.
Good, P. I. (2005), *Permutation, Parametric, and Bootstrap Tests of Hypotheses*, Springer, New York.
IPCC (2007), *Contribution of Working Groups I, II and III to the Fourth Assessment Report of the Intergovernmental Panel on Climate Change*, edited by B. Metz et al., Cambridge Univ. Press, Cambridge, U.K., and New York.
Janssens, I. A., et al. (2010), Reduction of forest soil respiration in response to nitrogen deposition, *Nat. Geosci.*, *3*(5), 315–322.
Kelly, R. H., W. J. Parton, M. D. Hartman, L. K. Stretch, D. S. Ojima, and D. S. Schimel (2000), Intra-annual and interannual variability of ecosystem processes in shortgrass steppe, *J. Geophys. Res.*, *105*(D15), 20,093–20,100.
Kooijman, A. M., M. M. Kooijman-Schouten, and G. B. Martinez-Hernandez (2008), Alternative strategies to sustain N-fertility in acid and calcaric beech forests: Low microbial N-demand versus high biological activity, *Basic Appl. Ecol.*, *9*(4), 410–421.
Lawrence, C. R., J. C. Neff, and J. P. Schimel (2009), Does adding microbial mechanisms of decomposition improve soil organic matter models? A comparison of four models using data from a pulsed rewetting experiment, *Soil Biol. Biochem.*, *41*(9), 1923–1934.
Leirós, M. C., C. Trasar-Cepeda, S. Seoane, and F. Gil-Sotres (1999), Dependence of mineralization of soil organic matter on temperature and moisture, *Soil Biol. Biochem.*, *31*(3), 327–335.
Lu, M., X. Zhou, Y. Luo, Y. Yang, C. Fang, J. Chen, and B. Li (2011), Minor stimulation of soil carbon storage by nitrogen addition: A meta-analysis, *Agric. Ecosyst. Environ.*, *140*(1-2), 234–244.
Manzoni, S., and A. Porporato (2007), A theoretical analysis of nonlinearities and feedbacks in soil carbon and nitrogen cycles, *Soil Biol. Biochem.*, *39*(7), 1542–1556.
Manzoni, S., and A. Porporato (2009), Soil carbon and nitrogen mineralization: Theory and models across scales, *Soil Biol. Biochem.*, *41*(7), 1355–1379.
Manzoni, S., R. B. Jackson, J. A. Trofymow, and A. Porporato (2008), The global stoichiometry of litter nitrogen mineralization, *Science*, *321*(5889), 684–686.
Manzoni, S., J. A. Trofymow, R. B. Jackson, and A. Porporato (2010), Stoichiometric controls on carbon, nitrogen, and phosphorus dynamics in decomposing litter, *Ecol. Monogr.*, *80*(1), 89–106.
Manzoni, S., P. Taylor, A. Richter, A. Porporato, and G. I. Ågren (2012), Environmental and stoichiometric controls on microbial carbon-use efficiency in soils, *New Phytol.*, *196*(1), 79–91.
McGuire, K. L., and K. K. Treseder (2010), Microbial communities and their relevance for ecosystem models: Decomposition as a case study, *Soil Biol. Biochem.*, *42*(4), 529–535.
Metherell, A. K., L. A. Harding, C. V. Cole, and W. J. Parton (1993), CENTURY soil organic matter model environment. Technical documentation agroecosystem version 4.0., 247 pp.
Ostle, N. J., et al. (2009), Integrating plant–soil interactions into global carbon cycle models, *J. Ecol.*, *97*(5), 851–863.
Parton, W. J., D. S. Schimel, C. V. Cole, and D. S. Ojima (1987), Analysis of factors controlling soil organic-matter levels in Great-Plains grasslands, *Soil Sci. Soc. Am. J.*, *51*(5), 1173–1179.
Parton, W. J., et al. (1993), Observations and modeling of biomass and soil organic matter dynamics for the grassland biome worldwide, *Global Biogeochem. Cycles*, *7*(4), 785–809.
Parton, W., et al. (2007), Global-scale similarities in nitrogen release patterns during long-term decomposition, *Science*, *315*(5810), 361–364.
Pietsch, S. A., and H. Hasenauer (2006), Evaluating the self-initialization procedure for large-scale ecosystem models, *Global Change Biol.*, *12*(9), 1658–1669.
Porporato, A., P. D'Odorico, F. Laio, and I. Rodriguez-Iturbe (2003), Hydrologic controls on soil carbon and nitrogen cycles. I. Modeling scheme, *Adv. Water Resour.*, *26*(1), 45–58.
Ramirez, K. S., J. M. Craine, and N. Fierer (2010), Nitrogen fertilization inhibits soil microbial respiration regardless of the form of nitrogen applied, *Soil Biol. Biochem.*, *42*(12), 2336–2338.
Rastetter, E. B., J. D. Aber, D. P. C. Peters, D. S. Ojima, and I. C. Burke (2003), Using mechanistic models to scale ecological processes across space and time, *BioScience*, *53*(1), 68–76.
Ros, G. H. (2012), Predicting soil N mineralization using organic matter fractions and soil properties: A re-analysis of literature data, *Soil Biol. Biochem.*, *45*, 132–135.
Ross, D. J., K. R. Tate, and C. W. Feltham (1996), Microbial biomass, and C and N mineralization, in litter and mineral soil of adjacent montane ecosystems in a southern beech (Nothofagus) forest and a tussock grassland, *Soil Biol. Biochem.*, *28*(12), 1613–1620.
Ross, D. J., K. R. Tate, N. A. Scott, and C. W. Feltham (1999), Land-use change: Effects on soil carbon, nitrogen and phosphorus pools and fluxes in three adjacent ecosystems, *Soil Biol. Biochem.*, *31*(6), 803–813.
Schimel, D. S. (1994), Climatic, edaphic, and biotic controls over storage and turnover of carbon in soils, *Global Biogeochem. Cycles*, *8*(3), 279–293.
Schimel, J. P., and J. Bennett (2004), Nitrogen mineralization: Challenges of a changing paradigm, *Ecology*, *85*(3), 591–602.
Schimel, J. P., and M. N. Weintraub (2003), The implications of exoenzyme activity on microbial carbon and nitrogen limitation in soil: A theoretical model, *Soil Biol. Biochem.*, *35*(4), 549–563.
Serna-Chavez, H. M., N. Fierer, and P. M. van Bodegom (2013), Global drivers and patterns of microbial abundance in soil, *Global Ecol. Biogeogr.*, *22*, 1162–1172.
Sinsabaugh, R. L., et al. (2008), Stoichiometry of soil enzyme activity at global scale, *Ecol. Lett.*, *11*, 1252–1264.
Sinsabaugh, R. L., S. Manzoni, D. L. Moorhead, and A. Richter (2013), Carbon use efficiency of microbial communities: Stoichiometry, methodology and modelling, *Ecol. Lett.*, *16*(7), 930–939.
Six, J., S. D. Frey, R. K. Thiet, and K. M. Batten (2006), Bacterial and fungal contributions to carbon sequestration in agroecosystems, *Soil Sci. Soc. Am. J.*, *70*(2), 555–569.
Thornton, P. E., J. F. Lamarque, N. A. Rosenbloom, and N. M. Mahowald (2007), Influence of carbon-nitrogen cycle coupling on land model response to CO_2 fertilization and climate variability, *Global Biogeochem. Cycles*, *21*, GB4018, doi:10.1029/2006GB002868.
Todd-Brown, K., F. Hopkins, S. Kivlin, J. Talbot, and S. Allison (2011), A framework for representing microbial decomposition in coupled climate models, *Biogeochemistry*, *109*(1-3), 19–33.
Todd-Brown, K. E. O., J. T. Randerson, W. M. Post, F. M. Hoffman, C. Tarnocai, E. A. G. Schuur, and S. D. Allison (2013), Causes of variation in soil carbon simulations from CMIP5 Earth system models and comparison with observations, *Biogeosciences*, *10*(3), 1717–1736.
Treseder, K., et al. (2012), Integrating microbial ecology into ecosystem models: challenges and priorities, *Biogeochemistry*, *109*(1-3), 7–18.

Whitmore, A. P. (1996), Describing the mineralization of carbon added to soil in crop residues using second-order kinetics, *Soil Biol. Biochem.*, *28*(10–11), 1435–1442.

Wieder, W. R., G. B. Bonan, and S. D. Allison (2013), Global soil carbon projections are improved by modelling microbial processes, *Nat. Clim. Change*, *3*(10), 909–912.

Wirth, S. J. (2001), Regional-scale analysis of soil microbial biomass and soil-basal CO2-respiration in northeastern Germany, in *Sustaining the Global Farm – Selected Papers From the 10th International Soil Conservation Organization Meeting, May 24-29, 1999, West Lafayette*, edited by D. E. Stott, R. H. Mohtar, and G. C. Steinhardt, pp. 486–493, International Soil Conservation Organization in cooperation with the USDA and Purdue University, West Lafayette, Ind.